ChemPubSoc Europe

DOI: 10.1002/cplu.201500218

CHEMPLUSCHEM Full Papers

VIP

Programming Bioactive Architectures with Cyclic Peptide Amphiphiles

Seah Ling Kuan,* Tao Wang, Marco Raabe, Weina Liu, Markus Lamla, and Tanja Weil*[a]

We present a versatile approach for the synthesis of cyclic peptide amphiphiles of the hormone somatostatin (SST) with tunable lipophilic tails to program bioactive nanoarchitectures. A novel bis-alkylation reagent is synthesized that facilitates the functionalization of SST with a thiol anchor. Different hydrophobic moieties are introduced inspired by a biomimetic palmitoylation approach which opens access to cyclic peptide amphiphiles that display rich self-organization and cell membrane interactions.

Introduction

The synthesis and design of peptide amphiphiles (PAs) has attracted considerable attention owing to various applications in biotechnology and biomedicine including drug delivery and regenerative medicine.[1–5] Peptide derivatives with amphiphilic properties due to alternating sequences of hydrophobic and hydrophilic (charged) residues that assemble into higher order nanostructures have been reported.[6–8] Additionally, peptides that are modified through the attachment of hydrophobic lipid chains have displayed unique self-assembly properties and have also been adopted as noncovalent anchors for insertion into nanocarriers such as liposomes.[9,10] In particular, the design of PAs with bioactive peptides as targeting ligands is highly attractive for the directed delivery of drugs or bioimaging agents.[10] Although the library of synthetic linear PAs is abundant in the literature, examples of synthetic cyclic PAs still remain scarce.[11–13]

Cyclic peptides play important roles in many cellular processes including cellular signaling. Moreover, they are known to be more stable and usually exhibit higher target-binding affinity than the corresponding linear counterparts due to their rigid scaffolds.[14] Cyclic lipopeptides comprising a cyclic peptide headgroup with a lipid tail are expressed by bacteria and display a rich pharmacology with antibacterial, antifungal, and antiviral activities.[15] Consequently, the functionalization of bioactive cyclic peptides that introduces new features for controlling bioactivity or self-assembly[13,16–20] could be valuable for many therapeutic applications.

Still, the site-directed attachment of hydrophobic moieties such as lipids to cyclic peptides and subsequent purification are challenging.[21,22] One of the few examples is the well-known cyclic RGDFK PA; it contains a dialkyl lipid chain attached to the cyclic peptide through the lysine ε-amino group.[23] This elegant approach requires the presence of only a single lysine residue that is not involved in the bioactivity of the peptide. Therefore, larger cyclic peptides with multiple lysines located in or close to the protein binding site cannot be modified by this reaction. As a result, there is a considerable interest in developing a synthetic PA platform by a more versatile chemical approach.

In the cellular machinery, posttranslation processes allow for the modification of proteins with lipids and one of the predominant modifications occurs at the free cysteine residue.[24] In this respect, the physiological palmitoylation machinery could serve as a good synthetic model for deriving amphiphilic cyclic peptides in a site-directed manner. Evaluation of protein databases shows that most therapeutically relevant polypeptides and proteins offer at least one disulfide bond close to the surface that is directed away from the active sites.[25] Many cyclic peptides found in nature such as somatostatin and oxytocin possess a single disulfide bridge that imparts stability and is often crucial for generating the correct bioactive three-dimensional architecture.[26,27] However, the presence of disulfide bridges in cyclic peptides often limits the possibilities to introduce additional free cysteine residues due to disulfide scrambling, which leads to wrongly folded nonactive peptides and thus reduces the yields during peptide expression and solid-phase synthesis.[28,29]

Herein, we report the synthesis of three cyclic PAs of the peptide hormone somatostatin (SST) whose amphiphilic properties are tuned in a versatile manner to tailor different bionanoarchitectures. SST is a neuropeptide that is efficiently taken

[a] Dr. S. L. Kuan,[+] Dr. T. Wang,[+] M. Raabe, W. Liu, Dr. M. Lamla, Prof. Dr. T. Weil
Institute of Organic Chemistry III–Macromolecular Chemistry & Biomaterials
Ulm University, Albert-Einstein-Allee 11
89081 Ulm (Germany)
E-mail: seah-ling.kuan@uni-ulm.de
tanja.weil@uni-ulm.de

[+] These authors contributed equally to this work.

Supporting information for this article is available on the WWW under http://dx.doi.org/10.1002/cplu.201500218. It contains experimental details and syntheses of compounds **1**, **3**–**5**.

Part of a Special Issue to celebrate Singapore's Golden Jubilee. To view the complete issue, visit: http://dx.doi.org/10.1002/cplu.v80.8.

up into cells and translocated into the cytosol. This is mediated by five G protein coupled membrane-bound receptors (SSTR1–5) that are overexpressed in several tumors including breast, lung, prostate, and neuroendocrine cancers.[30–32] SST derivatives can serve both as targeting ligands as well as antiproliferative drugs.[33,34] Due to their bioactivities, SST conjugates are of immense clinical interest for radiotherapy, tumor imaging, and chemotherapy.[35,36]

Results and Discussion

The functionalization of SST relies on the structurally novel bis-alkylation reagent 2-((*tert*-butoxycarbonyl)thio)ethyl 2-(tosylmethyl)acrylate (**3**), which introduces a single thiol anchor group by converting the chemically labile disulfide bond into two more stable bis-sulfides (Scheme 1). Bis-alkylation reagents have been used for the functionalization of peptide hormones,[37–39] antibodies,[25,40] oligonucleotides,[41] and therapeutic proteins.[40] In contrast to conventional bis-sulfone reagents containing three phenyl rings,[37] **3** offers improved solubility and the thiol anchor can be attached under aqueous conditions; various modifications with hydrophobic substituents can be introduced subsequently (Scheme 1 a).[42]

The bis-alkylation reagent **3** was synthesized by a multistep reaction sequence (Scheme 1 b, Supporting Information (SI)). *O*-(*tert*-butyl) *S*-(2-hydroxyethyl) carbonothioate (**1**) was first synthesized in 85% yield to protect the thiol group for subsequent reactions. Thereafter, **1** reacted with methacryloyl chloride to afford 2-((*tert*-butoxycarbonyl)thio)ethyl methacrylate (**2**) in 83% yield. Finally, **3** was obtained in 59% yield from the oxidation of **2** and sodium *p*-toluene sulfinate. Compound **3** contains a monosulfone group as the reactive species and can react with SST via two consecutive Michael additions in aqueous buffer.[42]

SST was first reduced at the disulfide by treatment with tris(2-carboxyethyl)phosphine hydrochloride (TCEP) in 50 mM phosphate buffer (PB) at pH 7.8 and then incubated with **3** overnight at room temperature. We postulated that **3** reacted with a free thiol group of the reduced disulfide, followed by the subsequent elimination of the *p*-toluenesulfinic acid group to form a second Michael system. In the presence of another thiol group in close vicinity, the second Michael addition occurred with the concomitant formation of a C_3-rebridged bis-sulfide.[40] The product was purified by HPLC and the Boc protecting group was removed by treatment with TFA/H_2O (2:1) for 1 h at room temperature to afford the thiol-functionalized SST, SST-SH (**4**) in 41% yield over two steps. Application of this method rather than the strategy of using conventional bis-sulfone reagent that we have reported previously[37] leads to an almost twofold increase in the yield of SST-SH due to the improved solubility of the bis-alkylation reagent in aqueous medium.

Thiol–maleimide chemistry is often employed in bioconjugation reactions due to fast reaction kinetics, atom efficiency, catalyst-free conditions, and the improved stability of the thioether addition product.[43,44] Thus, it is attractive to apply thiol–maleimide chemistry to program the amphilicity of cyclic peptides through a thiol anchor. Hydrophobic maleimide derivatives **6**–**8** were prepared by the reaction of *N*-(2-aminoethyl) maleimide trifluoroacetate salt (**5**) with either the NHS esters (Py-NHS, Pal-NHS) or the acid chloride (Cho-Cl) as depicted in Scheme 2 a in moderate to high yield (63–81%). The hydrophobic groups were selected for their different functions and lipophilicities, as determined from the calculated values of the octanol/water partition coefficients (log *P*(o/w)); hydrophobic character of the groups increased in the following order: pyrene < palmitoyl < cholesteryl (Table 1).

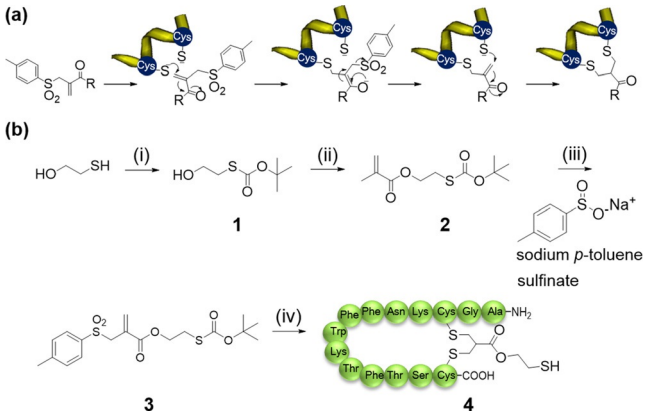

Scheme 1. Synthesis of SST-SH **4**. i) K_2CO_3, Boc_2O, ACN, 24 h, 85%; ii) Et_3N, methacryloyl chloride, anhydrous DCM, overnight, 83%; iii) I_2, sodium *p*-toluene sulfinate, DCM, 3 d, then 3 equiv Et_3N RT overnight and reflux overnight in EA, 59%; iv) SST, TCEP, 50 mM PB, pH 7.8, 24 h, then TFA/MiliQ H_2O (2:1), 1 h, 41%. ACN = acetonitrile, DCM = dichloromethane, EA = ethyl acetate, TCEP = (tris(2-carboxyethyl)phosphine), TFA = trifluoroacetic acid.

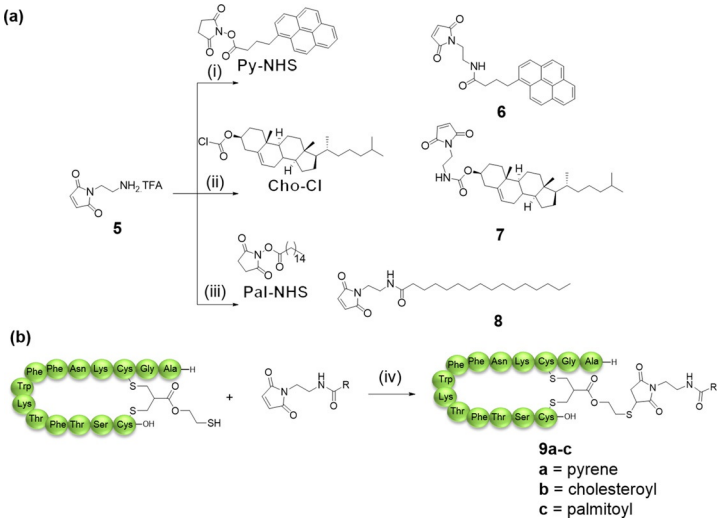

Scheme 2. a) Synthesis of hydrophobic maleimide derivatives **6**–**8**: i) pyrene-*N*-hydroxysuccinimide ester (Py-NHS), DIEA, DMF, RT, overnight, 81%; ii) cholesteryl chloroformate (Cho-Cl), DIEA, DMF/$CHCl_3$, RT, overnight, 63%; iii) palmitic acid *N*-hydroxysuccinimide ester (Pal-NHS), DIEA, DMF/$CHCl_3$, RT, overnight, 70%. b) Synthesis of somatostatin amphiphiles **9a**–**c** by a biomimetic approach: iv) maleimides **6**–**8**, DMF/$CHCl_3$, 48 h (56%, 23%, 69%, respectively). DIEA = *N*,*N*-diisopropylethylamine, DMF = dimethylformamide.

Table 1. log *P*(o/w) values obtained for SST and compounds **4**–**8**.

SST	**6**	**7**	**8**
−3.01	4.29	6.97	5.23
SST-SH (**4**)	**9a**	**9b**	**9c**
−3.24	0.43 (18.7)[a]	3.11 (20.1)[a]	1.36 (19.7)[a]

[a] HPLC retention time in min.

Pyrene has interesting photophysical properties due to the long lifetime of its monomers and the efficient formation of excimers;[45] peptides with this modification might provide a fluorescence probe for additional characterization and may also interact with hydrophobic drugs through π–π interactions for host–guest encapsulation. The two lipids cholesterol and palmitic acid are essential components in mammalian cell membranes and facilitate the insertion of bioactive peptide amphiphiles into nanocarriers such as liposomes and carrier proteins in a noncovalent fashion.[9,10] The resultant bioactive amphiphiles had been exploited as targeting ligands to modulate transport across biological barriers and the localization of the carrier inside tumor cells.[46]

The reaction of **4** with the respective hydrophobic maleimides (**6**–**8**) was carried out under argon atmosphere in dimethylformamide (DMF)/chloroform ($CHCl_3$) over 48 h to afford amphiphilic somatostatin analogues **9a**–**c** as shown in Scheme 2b. Cyclic peptide **9a** was obtained in 56% yield after purification and MALDI-TOF MS is in agreement with mass signals at 2194.92 $[M+H]^+$ (SI, Figure S4). Successful conjugation of pyrene in **9a** was further corroborated by the characteristic absorption of pyrene at 346 nm and its fluorescence emission spectrum (SI, Figure S5). Excimer formation of **9a** was observed at 0.25 wt% (2.5 mg mL^{-1}). Peptides **9b** and **9c** were obtained in about 23% and 69% yield, respectively, and were identified by MALDI-TOF MS (**9b**: 2337.14 $[M+H]^+$; **9c**: 2163.04 $[M+H]^+$).The calculated log *P*(o/w) values (Table 1) corroborate the HPLC retention times of the cyclic PAs and indicate that the hydrophobic character of the cyclic amphiphiles is strongly influenced by the hydrophobic units, increasing in the order: pyrene < palmitoyl < cholesteryl.

It had been demonstrated that SST conjugates prepared using a similar bis-alkylation scheme act as potent SSTR2 agonists and that they are internalized into MCF-7 cells which overexpress the SST receptors.[38] Thus, formation of a nanostructure with the SST PAs on the exterior could be important for therapeutic applications given the epitope's known bioactivity and was therefore further investigated. TEM images of **9a** at 0.5 wt% and 1 wt% showed that the spherical assemblies formed have more homogenous size distribution at 1 wt% with an average diameter of 265 ± 40 nm (Figure 1a–b, SI, Figure S10). The pyrene residue in **9a** is expected to localize within the hydrophobic compartment of the spherical assembly and interact with aromatic hydrophobic dyes such as Nile Red (NR). Following a literature protocol for encapsulation studies,[47] **9a** was then mixed with NR in a 1:1 mole ratio to form **9a**⊃NR. The NR fluorescence lifetime has been reported to decrease significantly with an increase in the hydrogen-bonding capability of the solvent.[45,48] At a **9a** concentration of 0.25 wt%, there was a sharp increase in fluorescence intensity upon the formation of the spherical assemblies which indicates the presence of NR within the hydrophobic compartments of the amphiphilic nanostructures (Figure 1c). In addition, a concomitant blue shift of the fluorescence emission (from 660 nm to 650 nm) and a nonradiative energy transfer (NRET) from the pyrene excimer to NR (Figure 1d) at λ_{ex} = 346 nm were also observed, indicating the close proximity of **9a** and NR which is a result of the encapsulation of NR in the hydrophobic compartments of the spherical assemblies.

The lipophilic tails of **9b** and **9c** can be employed as noncovalent anchors to arrange SST on the exterior of defined three-dimensional architectures of nanocarriers in order to direct and modulate their localization in cells. We have chosen human

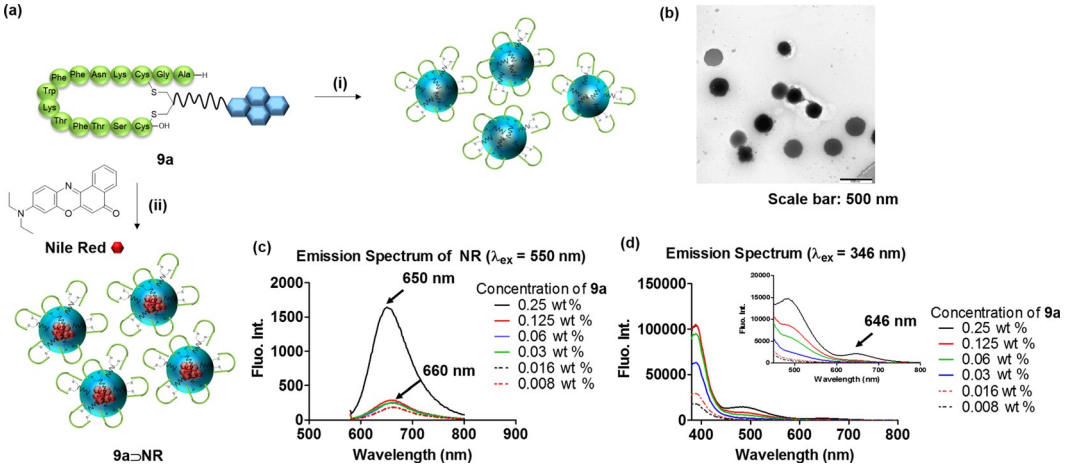

Figure 1. a) Schematic representation of the formation of spherical assemblies of **9a** and encapsulation of Nile Red (NR) dye. i) 1 wt% **9a** in H_2O from a 5 wt% solution of **9a** in DMSO and ii) 0.5 wt% **9a** and NR. b) TEM image of 1 wt% **9a**. Sample is stained with 2% sodium phosphotungstate adjusted to pH 7. c) Emission spectra of NR incubated with varying concentrations of **9a** showing incorporation of the hydrophobic dye at 0.25 wt%. d) Emission spectra of NR incubated **9a**. Inset shows NRET from excimer of **9a** to NR at higher concentration.

serum albumin (HSA) as the carrier core for the proposed system based on its biocompatibility. HSA is a natural transporter for various molecules and one of the most exploited proteins used as a drug delivery vehicle in therapeutics and clinical biochemistry.[49–53] It is known to be involved in transport and storage in biological processes and possesses hydrophobic binding pockets for both exogenous and endogenous ligands.[50,54] It has seven binding sites for fatty acids (Figure 2a)[55] and cholesterol has been shown to bind to HSA with

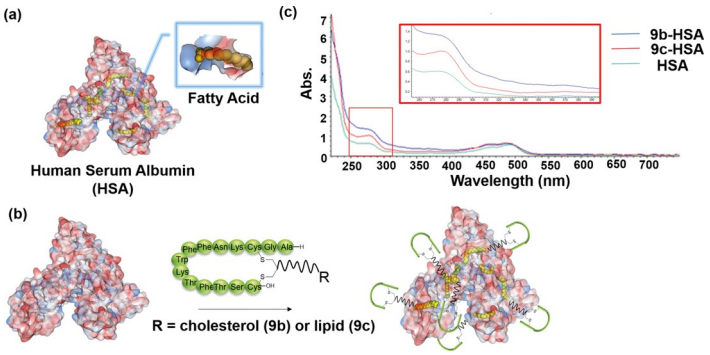

Figure 2. a) Human serum albumin and its binding sites for fatty acids. b) Binding **9b** and **9c** (10 mol equiv) to HSA (1 mol equiv), 3 h, RT. c) Absorbance spectra of HSA, **9b**-HSA, and **9c**-HSA showing successful binding. Inset depicts the expansion for absorbance at 280 nm. HSA used is fluorescein-labeled.

a K_b value on the order of 10^5.[54] This unique feature of HSA to bind hydrophobic molecules has been exploited clinically: ABRAXANE, an albumin-bound form of the antitumor drug paclitaxel, is currently available on the market as a drug for breast cancer treatment.[56] The combination of HSA with tumor-targeting groups and drugs is therefore highly promising for designing an efficient translational drug transporter.[49]

Compounds **9b** and **9c** were applied as noncovalent anchors that assembled SST at the periphery of HSA via the interaction of the lipid or cholesterol substituents with the protein's binding pockets (Figure 2b). An excess of **9b** or **9c** was added to fluorescein-labeled HSA and the mixture was incubated for 3 h. Thereafter, any unbound **9b** and **9c** was removed through ultrafiltration (molecular weight cut-off = 30 kDa) to afford the SST-loaded HSA analogues **9b**-HSA and **9c**-HSA. Figure 2c shows the absorbance spectra of **9b**-HSA, **9c**-HSA, and HSA with their concentrations normalized using the absorbance signal of fluorescein at 480 nm. The absorbance values at 280 nm for **9b**-HSA and **9c**-HSA are much higher than that of native HSA due to the additional contribution of aromatic amino acid residues from somatostatin. This supports the successful binding of **9b** and **9c** to HSA. This was further substantiated by agarose gel electrophoresis where a new band appeared for **9b**-HSA with lower mobility (Figure S12b) due to the increase in molecular weight and decrease in negative charge upon successful binding of the electropositive **9b** to HSA. The sizes of **9b**-HSA and **9c**-HSA as determined by dynamic light scattering (DLS) are 7.9 ± 1.1 nm and 6.4 ± 0.2 nm respectively (Table S1). The slight increase in size compared to native HSA (6.3 ± 1.0 nm) is presumably due to the binding of the somatostatin amphiphiles. An AFM study of **9c**-HSA shows single macromolecules with a height of 1.5 ± 0.4 nm which is comparable to HSA with a height of 1.4 ± 0.4 nm (Figure S13).

To investigate the bioactivity of the supramolecular SST towards SSTR-positive cell lines after modification, a cellular uptake assay was accomplished in the human breast cancer cell line MCF-7 which expresses the SSTR2 receptor.[33] After 2 h of incubation with **9a** the fluorescence emission of lysed MCF-7 was obtained as an indicator for successful membrane translocation. A concentration-dependent uptake of **9a** (Figure 3a) was observed and the translocation of **9a**⊃NR across cellular membranes was also substantiated by confocal microscopy (Figure 3b).

Next, we investigated the translocation of **9b**-HSA and **9c**-HSA across cell membranes in comparison to native HSA, which does not permeate membranes of non-inflamed tissue.[57,58] It was observed that the cyclic PAs **9b** and **9c** facilitate the transport of fluorescein-labeled HSA into cells (Figure 3d). Interestingly, **9b**-HSA was localized in the cell membranes while **9c**-HSA was internalized into the cells. The difference in the localization is presumably because the cholesterol moiety in **9b**-HSA directs the anchored HSA to the cholesterol-enriched domains, which are known to be highly expressed in tumor cells.[59,60] Cell uptake studies of **9a**, **9b**-HSA, and **9c**-HSA carried out at 4 °C and 37 °C were compared since receptor-mediated uptake is an energy-dependent process.[61] There is a significant inhibition of the cell uptake of **9a**, **9b**-HSA, and **9c**-HSA (Figure 3a,c) at 4 °C of 57% (average over all concentrations), 53% and 67%, respectively (Tables S2 and S3), thereby clearly indicating that **9a**, **9b**-HSA, and **9c**-HSA enter cells via receptor-mediated cell uptake rather than via passive diffusion.

Conclusion

Drawing inspiration from the cellular palmitoylation process, we have presented herein a two-step approach that allows the site-directed attachment of hydrophobic substituents in a convenient fashion in order to derive bioactive cyclic PAs 1) through the introduction of a thiol anchor to cyclic polypeptides and 2) capitalizing on the atom-efficient thiol–maleimide chemistry to achieve different lipid modifications. The peptide hormone SST was successfully functionalized with a thiol, and thus three different SST amphiphiles (**9a**–**9c**) were obtained from the SST-SH building block which complement the limited number of cyclic PAs in the literature. The SST amphiphiles were used to direct the assembly of different supramolecular bionanoarchitectures which could be used for drug delivery by encapsulating hydrophobic drugs with bioactive epitopes on the exterior as shown with **9a**. Or they could be employed to decorate the periphery of membrane impermeable proteins to facilitate their transport across cell membranes as shown with **9b** and **9c**. Notably, the SST amphiphiles **9a** and **9c** retain their SST bioactivity while the interaction of **9b** with cell membranes is seemingly dictated by the cholesterol group. Further

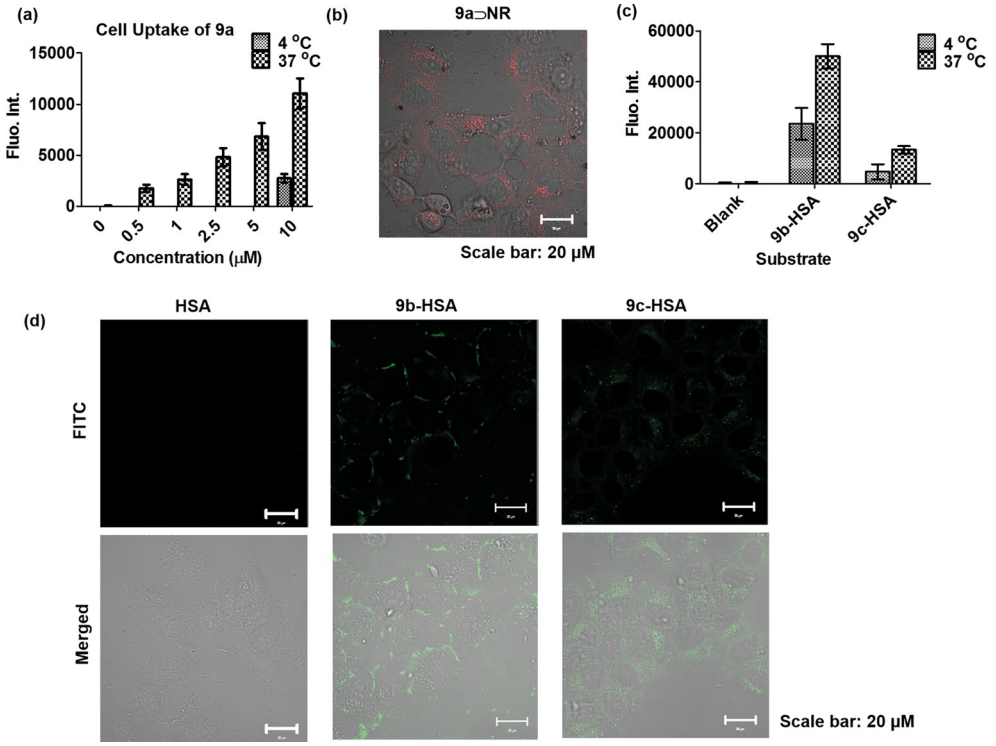

Figure 3. a) Uptake of **9a** into MCF-7 cells, 2 h incubation, 37 °C. Comparison of uptake of **9a** into MCF-7 cells (10 μM) showed 75% inhibition at 4 °C. b) Confocal images of NR and **9a**⊃NR in MCF-7 cells, 4 h incubation. c) Comparison of uptake of **9b**-HSA and **9c**-HSA (1 μM) into MCF-7 cells at 4 °C and 37 °C, 2 h incubation, with 53% and 65% inhibition, respectively. d) Confocal images of NR and **9b**-HSA, **9c**-HSA, and HSA in MCF-7 cells, 4 h incubation.

investigation should be undertaken to evaluate the influence of the lipid residue on the subcellular localization of nanocarriers. Based on these studies, new strategies for the design of bionanomaterials that can be directed to various subcellular localizations for targeted drug transport could be evolved. One can envision that the chemical amphiphile approach presented herein represents a versatile platform with significant potential to chemically program various cyclic peptides through self-organization to direct drug molecules or imaging reagents to specific cellular compartments in order to achieve efficient targeting at the subcellular level, which is of great interest in biomedicine and bioimaging.

Experimental Section

Synthesis of SST-SH (4)

Somatostatin (SST, 40 mg, 24.4 μmol) was dissolved in 35 mL of phosphate buffer (PB, 50 mM, pH 7.8) and TCEP (14 mg, 48.8 μmol) in 1 mL PB (50 mM, pH 7.8) was added. To this solution, compound **3** (19 mg, 48.8 μmol) in 24 mL of acetonitrile (ACN) was added slowly. The resulting reaction mixture was incubated at RT for 24 h. The mixture was then concentrated and purified by Agilent 1260 HPLC using a LiChrospher 100, RP-18, 10 μm, LiChroCART 250–10 column with the mobile phase starting at 95% solvent A (0.1% TFA in water) and 5% solvent B (0.1% TFA in ACN), increasing to 30% B at 5 min, further increasing to 80% B at 10 min, reaching 95% B at 22 min, maintained at 95% B for 3 min, and finally returning to 5% B at 30 min; the column was then equilibrated for 2 min with a flow rate of 4 mL min^{-1}. The absorbance was monitored at 280 nm and 220 nm. The product was dried by lyophilization and redissolved in 3 mL of TFA/MilliQ H_2O 2:1. The solution was stirred for 1 h at RT and 18 mg of the SST-SH **4** was obtained after lyophilization in 41% yield and characterized by MALDI-TOF-MS (m/z = 1783.7583 $[M+H]^+$). $C_{82}H_{114}N_{18}O_{21}S_3$. Calc. 1783.75915 $[M+H]^+$.

Synthesis of somatostatin amphiphiles (9a–c)

All manipulation and reactions were carried out under argon. To a solution of SST-SH (**4**) dissolved in anhydrous DMF at a concentration of about 1 mg mL^{-1} was added 10 mol equiv of the respective maleimides (**6**–**8**) dissolved in anhydrous DMF (**6**) or $CHCl_3$ (**7**, **8**) at a concentration of ca. 5 mg mL^{-1} and the reaction mixture was left to stir for 48 h at RT. The solvent was removed under reduced pressure and the solid was washed with 3×2 mL DCM to remove unreacted **6**–**8** to yield **9a–c**. The resultant residue was then purified by HPLC for the SST amphiphiles **9a**,**b**. All the products were characterized by MALDI-MS or LC-MS.

9a: MALDI-TOF MS: 2194.92010 $[M+H]^+$; ESI-MS: 1098 $[M+2H]^{2+}$; 731 $[M]^{3+}$. Chemical formula: $C_{108}H_{136}N_{20}O_{24}S_3$, exact mass: 2194.93009 $[M+H]^+$.

9b: MALDI-TOF MS: 2337.14319 $[M+H]^+$; ESI-MS: 1169 $[M+2H]^{2+}$, 779 $[M]^{3+}$. Chemical formula: $C_{116}H_{166}N_{20}O_{25}S_3$, exact mass: 2337.15979 $[M+H]^+$.

9c: ESI-MS: 1082 $[M+2H]^{2+}$; 721 $[M]^{3+}$; MALDI-TOF MS: 2163.0415 $[M+H]^+$. Chemical formula: $C_{116}H_{166}N_{20}O_{25}S_3$, exact mass: 2163.0052 $[M+H]^+$. HPLC purity: 81%.

Transmission electron microscopy (TEM)

Holey carbon coated TEM grids were treated with 2 μL of 1 wt% or 0.5 wt% **9a**, washed with water to remove excess material, and negatively stained with 2 wt% aqueous sodium phosphotungstate acid adjusted to pH 7. The TEM samples were air-dried overnight prior to imaging.

Encapsulation of Nile Red (NR) with 9a

In this experiment 1 μL of Nile Red (22.8 mM in $CHCl_3$/MeOH, 4:1) was mixed with 1 μL of **9a** (5 wt% in DMSO) and the volatile solvent was allowed to evaporate. Thereafter, water was added to reach a total volume of 10 μL (0.5 wt% **9a**) and the mixture was incubated for 30 min at RT. The solution was diluted to 20 μL (0.25 wt% **9a**) for absorbance and fluorescent measurements. Six serial dilutions of **9a** were also made from 5 wt% to show the difference in encapsulation of NR. Fluorescence spectra were obtained at λ_{ex} = 346 nm and 550 nm.

Binding of 9b or 9c to human serum albumin

In this experiment 10 mol equiv of **9b** or **9c** was added to 0.5 mg of FITC-labeled HSA in water and the mixture was incubated for 3 h. Thereafter, excess **9b** and **9c** was removed by ultrafiltration three times against water using Vivaspin 500 Centrifugal Concentrator (molecular weight cut-off = 30 kDa). Protein concentration was determined by comparison of the absorbance at λ = 480 nm against that of a standard solution of FITC-labeled HSA (0.5 mg mL^{-1}).

Cell culture

MCF-7 cells, a human breast cancer cell line, were cultured in high-glucose DMEM supplemented with 10% fetal bovine serum (FBS), 100 U mL^{-1} penicillin, 0.1 mg mL^{-1} streptomycin, and 0.1 mM non-essential amino acids at 37 °C in a humidified 5% CO_2 incubator. MCF-7 cells were plated into a white 96-well half-area microplate at a density of 3000 cells (24 h) per well in 50 μL complete DMEM and incubated overnight for attachment. For cell studies at 4 °C, the cells were preincubated for 30 min at 4 °C before addition of substrates. All measurements were performed in triplicate.

Cell uptake

After cell attachment, **9a** (50 μL each of 0 μM, 1 μM, 2.5 μM, 5 μM, 10 μM), **9b**-HSA, or **9c**-HSA (50 μL each of 1 μM) in fresh medium was applied to cells and was incubated for 2 h at 4 °C or 37 °C. The cells were then washed two times with ice-cold PBS (50 μL) to remove the non-internalized samples and lysed with 50 μL of lysis buffer (50 mM Tris, 0.8% Triton, 0.2% SDS, pH 7.4) and incubated at RT for 5 h. The cell uptake was determined from the fluorescence of the lysate using a TECAN Infinite M1000 microplate reader (**9a**: λ_{ex} = 344 nm and λ_{em} = 400 nm; **9b**-HSA/**9c**-HSA: λ_{ex} = 488 nm and λ_{em} = 520 nm).

Confocal microscopy

MCF-7 cells were were plated in a Coverglass Lab-Tek 8-well chamber (Nunc, Denmark) at a density of 30000 cells per well in 300 μL DMEM. The cells were incubated for overnight at 37 °C in 5% CO_2 to allow adhesion. Samples were prepared according to the description in the Supporting Information. Imaging was then performed using a LSM 710 laser scanning confocal microscope system (Zeiss, Germany) coupled to an XL-LSM 710 S incubator and equipped with a 63× oil immersion objective. The acquired images were processed with Zen software developed by Carl Zeiss.

Acknowledgements

We are grateful for financial support from the ERC Synergy (grant 319130-BioQ) and the Volkswagen Foundation (grant number Akz 86 366). We thank Stephan Fischer for technical support and Andrew Norris and Adewola Osunsade for proofreading.

Keywords: peptide amphiphiles · supramolecular bioconjugates · protein nanoarchitecture · somatostatin

[1] H. Cui, M. J. Webber, S. I. Stupp, *Pept. Sci.* **2010**, *94*, 1 – 18.
[2] N. Wiradharma, Y. W. Tong, Y. Y. Yang, *Macromol. Rapid Commun.* **2010**, *31*, 1212 – 1217.
[3] J.-X. Chen, H.-Y. Wang, C.-Y. Quan, X.-D. Xu, X.-Z. Zhang, R.-X. Zhuo, *Org. Biomol. Chem.* **2010**, *8*, 3142 – 3148.
[4] C. Valéry, F. Artzner, M. Paternostre, *Soft Matter* **2011**, *7*, 9583 – 9594.
[5] D. Jiao, J. Geng, X. J. Loh, D. Das, T. C. Lee, O. A. Scherman, *Angew. Chem. Int. Ed.* **2012**, *51*, 9633 – 9637; *Angew. Chem.* **2012**, *124*, 9771 – 9775.
[6] C. C. Decandio, E. R. Silva, I. W. Hamley, V. Castelletto, M. S. Liberato, V. X. Oliveira, C. L. P. Oliveira, W. A. Alves, *Langmuir* **2015**, *31*, 4513 – 4523.
[7] X. D. Xu, C. S. Chen, B. Lu, S. X. Cheng, X. Z. Zhang, R. X. Zhuo, *J. Phys. Chem. B* **2010**, *114*, 2365 – 2372.
[8] I. W. Hamley, A. Dehsorkhi, V. Castelletto, *Langmuir* **2013**, *29*, 5050 – 5059.
[9] C.-W. Chen, D.-W. Lu, M.-K. Yeh, C.-Y. Shiau, C.-H. Chiang, *Int. J. Nanomed.* **2011**, *6*, 2567 – 2580.
[10] D. K. Chang, C. Y. Chiu, S. Y. Kuo, W. C. Lin, A. Lo, Y. P. Wang, P. C. Li, H. C. Wu, *J. Biol. Chem.* **2009**, *284*, 12905 – 12916.
[11] D. Oh, S. A. Darwish, A. N. Shirazi, R. K. Tiwari, K. Parang, *ChemMedChem.* **2014**, *9*, 2449 – 2453.
[12] S. Fernandez-Lopez, H. S. Kim, E. C. Choi, M. Delgado, J. R. Granja, A. Khasanov, K. Kraehenbuehl, G. Long, D. A. Weinberger, K. M. Wilcoxen, M. R. Ghadiri, *Nature* **2001**, *412*, 452 – 455.
[13] E. K. Chung, E. Lee, Y. B. Lim, M. Lee, *Chem. Eur. J.* **2010**, *16*, 5305 – 5309.
[14] E. M. Driggers, S. P. Hale, J. Lee, N. K. Terrett, *Nat. Rev. Drug Discovery* **2008**, *7*, 608 – 624.
[15] I. W. Hamley, *Chem. Commun.* **2015**, *51*, 8574 – 8583.
[16] Y. Loo, S. Zhang, C. A. E. Hauser, *Biotechnol. Adv.* **2012**, *30*, 593 – 603.
[17] A. R. Cormier, X. Pang, M. I. Zimmerman, H. X. Zhou, A. K. Paravastu, *ACS Nano* **2013**, *7*, 7562 – 7572.
[18] L. Li, H. Zhan, P. Duan, J. Liao, J. Quan, Y. Hu, Z. Chen, J. Zhu, M. Liu, Y. D. Wu, J. Deng, *Adv. Funct. Mater.* **2012**, *22*, 3051 – 3056.
[19] M. G. J. ten Cate, N. Severin, H. G. Boerner, *Macromolecules* **2006**, *39*, 7831 – 7838.
[20] R. J. Brea, C. Reiriz, J. R. Granja, *Chem. Soc. Rev.* **2010**, *39*, 1448 – 1456.
[21] J. T. Mika, G. Moiset, A. D. Cirac, L. Feliu, E. Bardají, M. Planas, D. Sengupta, S. J. Marrink, B. Poolman, *Biochim. Biophys. Acta Biomembr.* **2011**, *1808*, 2197 – 2205.
[22] A. Clausell, F. Rabanal, M. Garcia-Subirats, M. a. Alsina, Y. Cajal, *Luminescence* **2005**, *20*, 117 – 123.
[23] V. Marchi-Artzner, B. Lorz, C. Gosse, L. Jullien, R. Merkel, H. Kessler, E. Sackmann, *Langmuir* **2003**, *19*, 835 – 841.
[24] M. J. Nadolski, M. E. Linder, *FEBS J.* **2007**, *274*, 5202 – 5210.
[25] S. Brocchini, A. Godwin, S. Balan, J.-W. Choi, M. Zloh, S. Shaunak, *Adv. Drug Delivery Rev.* **2008**, *60*, 3 – 12.
[26] W. Tegge, W. Bautsch, R. Frank, *J. Pept. Sci.* **2007**, *13*, 693 – 699.
[27] A. Ortiz-Acevedo, G. R. Dieckmann, *Tetrahedron Lett.* **2004**, *45*, 6795 – 6798.

[28] H. T. He, R. N. Gürsoy, L. Kupczyk-Subotkowska, J. Tian, T. Williams, T. J. Siahaan, *J. Pharm. Sci.* **2006**, *95*, 2222 – 2234.
[29] L. Eldjarn, A. Pihl, *J. Am. Chem. Soc.* **1957**, *79*, 4589 – 4593.
[30] J. A. Koenig, R. Kaur, I. Dodgeon, J. M. Edwardson, P. P. Humphrey, *Biochem. J.* **1998**, *336*, 291 – 298.
[31] R. Cescato, S. Schulz, B. Waser, V. Eltschinger, J. E. Rivier, H.-J. Wester, M. Culler, M. Ginj, Q. Liu, A. Schonbrunn, J. C. Reubi, *J. Nucl. Med.* **2006**, *47*, 502 – 511.
[32] E. J. Rolleman, P. P. M. Kooij, W. W. De Herder, R. Valkema, E. P. Krenning, M. De Jong, *Eur. J. Nucl. Med. Mol. Imaging* **2007**, *34*, 1854 – 1860.
[33] M. Volante, R. Rosas, E. Allìa, R. Granata, A. Baragli, G. Muccioli, M. Papotti, *Mol. Cell. Endocrinol.* **2008**, *286*, 219 – 229.
[34] G. Weckbecker, R. Liu, L. Tolcsvai, C. Bruns, *Cancer Res.* **1992**, *52*, 4973 – 4978.
[35] F. Barbieri, A. Bajetto, A. Pattarozzi, M. Gatti, R. Würth, S. Thellung, A. Corsaro, V. Villa, M. Nizzari, T. Florio, *Int. J. Pept.* **2013**, *2013*, 926295.
[36] C. Grötzinger, B. Wiedenmann, *Ann. N. Y. Acad. Sci.* **2004**, *1014*, 258 – 264.
[37] T. Wang, Y. Wu, S. L. Kuan, O. Dumele, M. Lamla, D. Y. W. Ng, M. Arzt, J. Thomas, J. O. Mueller, C. Barner-Kowollik, T. Weil, *Chem. Eur. J.* **2015**, *21*, 228 – 238.
[38] T. Wang, D. Y. W. Ng, Y. Wu, J. Thomas, T. TamTran, T. Weil, *Chem. Commun.* **2014**, *50*, 1116 – 1118.
[39] A. Pfisterer, K. Eisele, X. Chen, M. Wagner, K. Müllen, T. Weil, *Chem. Eur. J.* **2011**, *17*, 9697 – 9707.
[40] S. Shaunak, A. Godwin, J.-W. Choi, S. Balan, E. Pedone, D. Vijayarangam, S. Heidelberger, I. Teo, M. Zloh, S. Brocchini, *Nat. Chem. Biol.* **2006**, *2*, 312 – 313.
[41] T. Wang, A. Pfisterer, S. L. Kuan, Y. Wu, O. Dumele, M. Lamla, K. Muellen, T. Weil, K. Mullen, T. Weil, *Chem. Sci.* **2013**, *4*, 1889 – 1894.
[42] S. Brocchini, S. Balan, A. Godwin, J.-W. Choi, M. Zloh, S. Shaunak, *Nat. Protoc.* **2006**, *1*, 2241 – 2252.
[43] E. M. Sletten, C. R. Bertozzi, *Angew. Chem. Int. Ed.* **2009**, *48*, 6974 – 6998; *Angew. Chem.* **2009**, *121*, 7108 – 7133.
[44] B. D. Mather, K. Viswanathan, K. M. Miller, T. E. Long, *Prog. Polym. Sci.* **2006**, *31*, 487 – 531.
[45] G. Nizri, S. Magdassi, *J. Colloid Interface Sci.* **2005**, *291*, 169 – 174.
[46] I. Haralampiev, M. Mertens, R. Schwarzer, A. Herrmann, R. Volkmer, P. Wessig, P. Müller, *Angew. Chem. Int. Ed.* **2015**, *54*, 323 – 326; *Angew. Chem.* **2015**, *127*, 328 – 332.
[47] M. O. Guler, R. C. Claussen, S. I. Stupp, *J. Mater. Chem.* **2005**, *15*, 4507 – 4512.
[48] S. Mukherjee, H. Raghuraman, A. Chattopadhyay, *Biochim. Biophys. Acta Biomembr.* **2007**, *1768*, 59 – 66.
[49] B. Elsadek, F. Kratz, *J. Controlled Release* **2012**, *157*, 4 – 28.
[50] R. Hussain, G. Siligardi, *Int. J. Pept. Res. Ther.* **2006**, *12*, 311 – 315.
[51] Y. Li, K. Xiao, J. Luo, J. Lee, S. Pan, K. S. Lam, *J. Controlled Release* **2010**, *144*, 314 – 323.
[52] S. L. Kuan, Y. Wu, T. Weil, *Macromol. Rapid Commun.* **2013**, *34*, 380 – 392.
[53] D. Y. W. Ng, Y. Wu, S. L. Kuan, T. Weil, *Acc. Chem. Res.* **2014**, *47*, 3471 – 3480.
[54] X. Tao, Q. Zhang, W. Yang, Q. Zhang, *Curr. Nanosci.* **2012**, *8*, 830 – 837.
[55] D. Charbonneau, M. Beauregard, H.-A. Tajmir-Riahi, *J. Phys. Chem. B* **2009**, *113*, 1777 – 1784.
[56] F. Kratz, *J. Controlled Release* **2008**, *132*, 171 – 183.
[57] J. R. Levick, *Arthritis Rheum.* **1981**, *24*, 1550 – 1560.
[58] A. Wunder, U. Müller-Ladner, E. H. K. Stelzer, J. Funk, E. Neumann, G. Stehle, T. Pap, H. Sinn, S. Gay, C. Fiehn, *J. Immunol.* **2003**, *170*, 4793 – 4801.
[59] R. Tiwary, W. Yu, L. A. deGraffenried, B. G. Sanders, K. Kline, *Breast Cancer Res.* **2011**, *13*, R120.
[60] R. C. Allsopp, U. Lalo, R. J. Evans, *J. Biol. Chem.* **2010**, *285*, 32770 – 32777.
[61] D. Pesce, Y. Wu, A. Kolbe, T. Weil, A. Herrmann, *Biomaterials* **2013**, *34*, 4360 – 4367.

Received: May 9, 2015
Published online on July 14, 2015